ELSEVIER

International Journal of Mass Spectrometry 198 (2000) 33–44

International Journal of Mass Spectrometry

Ab initio calculations on the isomerization and dissociation of C_4H_5N radical cations

W.J. van der Hart

Leiden Institute of Chemistry, Gorlaeus Laboratories, Leiden University, P. O. Box 9502, 2300 RA Leiden, The Netherlands

Received 11 October 1999; accepted 29 November 1999

Abstract

Ab initio calculations at the multireference configuration interaction/restricted open-shell Hartree-Fock/double zeta plus polarization level are performed on hydrogen shifts in the pyrrole radical cation, on dissociation to the CH_2CNH fragment ion and on possible pathways for the isomerization of allyl cyanide, crotonitrile, methacrylonitrile, and cyclopropyl cyanide radical cations. The barriers for hydrogen shifts in the pyrrole radical cation are significantly below the dissociation limit. The calculated dissociation limit of 3.69 eV is in reasonable agreement with the experimental value of 3.43 eV. The barrier for an isomerization of the other C_4H_5N radical cations to the pyrrole structure is calculated to be 4.10 eV, thus being higher than the dissociation limit. This implies that the formation of stable pyrrole radical cation from the other precursors, observed previously, should be ascribed to infrared radiative stabilization. The calculations on the isomerization as a whole are in good agreement with previous photodissociation experiments with a clear exception for the cyclopropyl cyanide radical cation. (Int J Mass Spectrom 198 (2000) 33–44) © 2000 Elsevier Science B.V.

Keywords: Ab initio calculations; C_4H_5N radical cations; Isomerization processes; Dissociation processes

1. Introduction

From previous studies of the mass spectra of a number of different precursors it has been concluded that C_4H_5N radical cations isomerize to a common structure, prior to fragmentation [1–3]. This common structure presumably is the pyrrole radical cation. The lowest dissociation channel is the loss of ethyne and the resulting fragment ion is assumed to have the $CH_2CNH^{\cdot+}$ structure [1,2]. The dissociation limit for this process is 3.43 eV [2].

From photodissociation studies of nonfragmenting C_4H_5N radical cations at an ionizing energy of 16 eV [4], it was subsequently concluded that ions from pyrrole and methacrylonitrile retain the structure of the neutral molecule and that ions from cyclopropyl cyanide and crotonitrile isomerize to the pyrrole structure for 15% and 6%, respectively. Finally, ionization of allyl cyanide leads to a mixture of three ion structures: allyl cyanide (25%), crotonitrile (45%), and pyrrole (30%).

In the present work these processes are studied by ab initio calculations. The reason for choosing this system is the close similarity of the different reactions with the isomerization of C_6H_6 radical cations [5–8] and of alkene radical cations [9] studied before by ab initio calculations.

* Corresponding author. E-mail: w.hart@chem.leidenuniv.nl

PII S1387-3806(99)00268-7

2. Methods

Ab initio calculations using Dunning and Huzinaga's double zeta plus polarization (DZP) basis set [10] were performed with both the GAMESS-UK [11] and the GAUSSIAN 94 [12] program packages. In previous calculations on the isomerization of radical cations we found that at crucial points on the potential energy surface an unrestricted Hartree-Fock (UHF) calculation may produce unacceptable values for the spin angular momentum (S^2) as high as 1.0. For this reason stable ion structures and transition states were optimized at the restricted open shell Hartree-Fock (ROHF) level. Transition states were tested by a calculation of the vibrational frequencies and by a visualization of the vibration corresponding with the single negative force constant by use of VIBRAM [13]. For the optimized structures, multireference configuration interaction (MRCI) calculations with single and double excitations were done with the Table CI (From [14], and references cited therein) option of GAMESS-UK. In these calculations, excitations involving the lowest 8 occupied and the highest 20 virtual molecular orbitals were not included. All configurations having a coefficient squared higher than 0.0025 in the final ground state wave function or higher than 0.0030 in the wave function for the second root (of the same symmetry) were used as reference configurations. The selection threshold used in Table CI was set at 3.0 μHartree. This implies that the number of configurations in the final diagonalization was in the order of 60 000. In the Table CI calculations, the contribution of the remaining configurations is calculated by perturbation theory. The final MRCI values given in the Tables include a generalized Davidson size-consistency correction [15].

In some cases transition states were optimized at the complete active space self-consistent field (CASSCF) level. An example is the isomerization of the substituted trimethylene radical cation **18** to the allyl cyanide structure **15** (see Fig. 4) where a hydrogen shifts from the central carbon atom to the carbon atom carrying the unpaired electron (Sec. 3.3). Just as in the calculations on the isomerization of alkene radical cations [9], an optimization of the geometry of the transition state was in this case only possible after a switch from ROHF to a CASSCF calculations. After this calculation the final wave function appeared to be close to a single Slater determinant. In order to keep the results as comparable as possible, the subsequent MRCI calculations were done with ROHF molecular orbitals.

3. Results and discussion

Similar to the case of C_6H_6 radical cations [5–8], one may assume that isomerizations of the C_4H_5N radical cations, mentioned in Sec. 1, to the pyrrole structure proceed via one or more ion structures obtained from the pyrrole radical cation by hydrogen shifts. Because the fragment ion obtained by loss of ethyne is assumed to have the $CH_2CNH^{\cdot+}$ structure [1,2], it also seems necessary that dissociation of the pyrrole radical cation is preceded by a hydrogen shift. For this reason, we will first consider hydrogen shifts in the pyrrole radical cation. This is followed by a discussion of possible pathways for the formation of the $CH_2CNH^{\cdot+}$ fragment ion and for isomerizations of the ions from the other precursors.

3.1. Hydrogen shifts in the pyrrole radical cation

The reaction scheme considered is shown in Fig. 1 and the results are summarized in Table 1. Fig. 1 also shows the relative energies in kcal mol^{-1} at the MRCI level after correction for the ZPE. In this reaction scheme possible shifts via structures with two hydrogen atoms on the nitrogen atom are not included. In these structures, the formal charge is localized on the nitrogen atom and the unpaired electron will be localized in a σ orbital on a carbon atom without a hydrogen. From this one should expect the energy of these structures and the barriers for a hydrogen shift to one of these structures to be higher than those included in Fig. 1. Because preliminary calculations showed that this is indeed the case, these structures were neglected in the further calculations. Besides, it

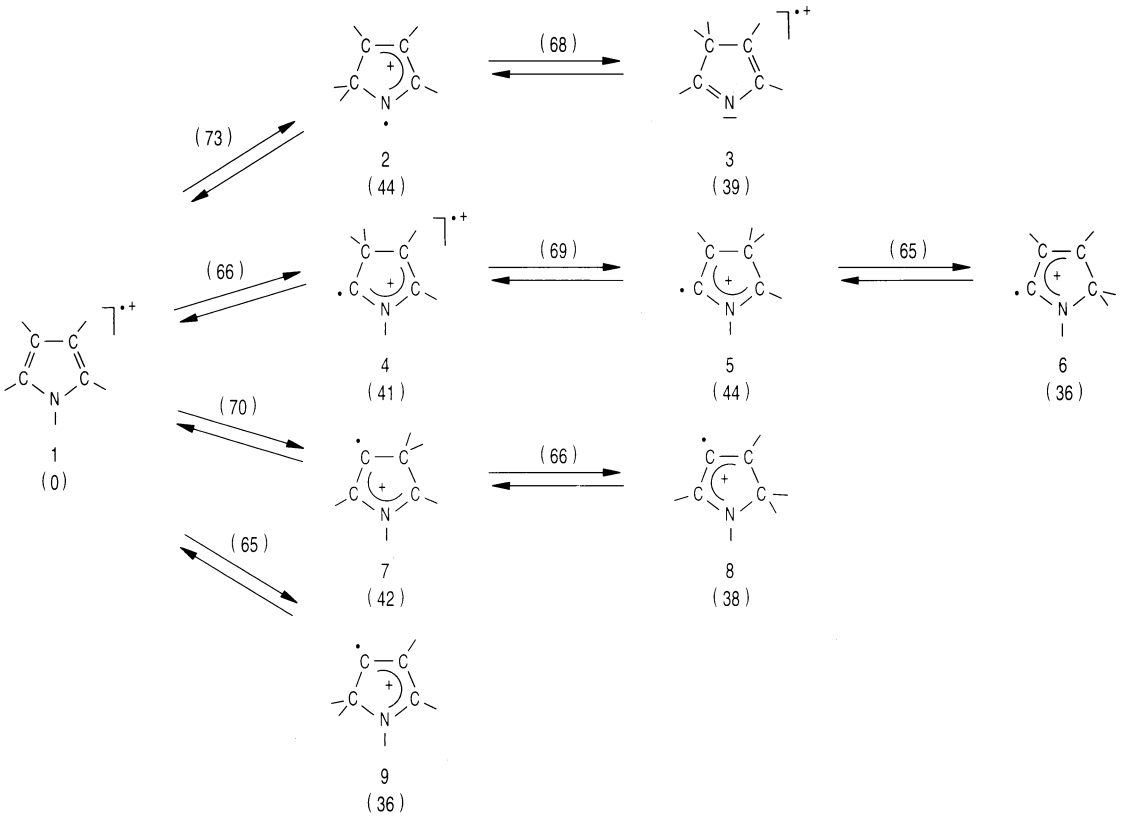

Fig. 1. Reaction scheme for hydrogen shifts in the pyrrole radical cation.

seems very unlikely that structures of this type will be intermediates in the isomerizations considered.

The highest barrier in Fig. 1 has a relative energy of 73 kcal mol^{-1} = 3.17 eV. This value is below the experimental dissociation limit of 3.43 eV [2]. It thus follows that, just as in the case of the benzene radical cation [5], the hydrogen atoms will be fully scrambled in dissociation processes.

3.2. Dissocation to the CH_2CNH radical cation

As noted in Sec. 1, the dissociation of lowest energy of the pyrrole radical cation leads to the loss of ethyne and formation of the CH_2CNH fragment ion. The most reasonable pathway for this process seems to be a hydrogen shift to structure **4** followed by a cleavage of first a C–N bond and then a C–C bond via structure **10** or vice versa via structure **11** (see Fig. 2). As shown in Table 2 and Fig. 2, the pathway via **10** clearly has the lowest energy. The final dissociation of both **10** and **11** proceeds via a minimum that should be ascribed to the ion induced dipole attraction. The relative orientation of the two fragments is different in the two cases and the energy of the minimum is lowest for dissociation of structure **11** (Table 2). Because the internal energy during dissociation will be higher than a possible barrier between the two minima, we will include the lowest energy minimum in the energy diagram for dissociation of the pyrrole radical cation via structure **10** (Fig. 3). The highest barrier in the fragmentation pathway is that for dissociation of structure **10**: 85.2 kcal mol^{-1} = 3.69 eV, which is somewhat higher than the experimental value of 3.43 eV = 79.1 kcal mol^{-1} [2]. It should be noted that most of the other barriers in Figs. 2 and 3 (and in Figs. 4 and 7) involve hydrogen shifts which

Table 1
ROHF, ZPE, and MRCI energies of the different radical cation structures and transition states in Fig. 1 and relative MRCI energies in kcal mol^{-1} corrected for the ZPE at the ROHF level scaled by a factor of 0.89

	ROHF	ZPE	MRCI	ΔE
Pyrrole **1**	−208.596 547	0.087 854	−209.052 045	0
2	−208.532 001	0.086 294	−208.979 764	44.5
3	−208.547 039	0.086 466	−208.988 220	39.3
4	−208.535 616	0.087 778	−208.986 604	41.0
5	−208.530 548	0.088 169	−208.982 951	43.5
6	−208.548 562	0.088 235	−208.995 278	35.8
7	−208.533 311	0.088 406	−208.985 213	42.2
8	−208.543 470	0.088 900	−208.992 369	38.0
9	−208.547 037	0.088 814	−208.995 981	35.7
$T_{1,2}$	−208.469 566	0.081 817	−208.930 327	73.0
$T_{2,3}$	−208.490 597	0.082 933	−208.939 332	68.0
$T_{1,4}$	−208.489 398	0.084 201	−208.943 475	66.1
$T_{4,5}$	−208.476 515	0.084 479	−208.938 589	69.3
$T_{5,6}$	−208.491 412	0.084 584	−208.945 020	65.3
$T_{1,7}$	−208.477 131	0.084 487	−208.938 134	69.7
$T_{7,8}$	−208.489 223	0.085 007	−208.944 324	66.0
$T_{1,9}$	−208.491 429	0.084 432	−208.944 628	65.5

means that experimental values (if these can be obtained) may be somewhat lower than calculated values because of tunneling.

3.3. Isomerization reactions of the other C_4H_5N radical cations

The most straightforward connection between one of the structures **2**–**9** in Fig. 1 and the other C_4H_5N radical cations studied (allyl cyanide **15**, crotonitrile **17**, methacrylonitrile **21**, and cyclopropyl cyanide **20**), seems to be the isomerization of the allyl cyanide radical cation **15** via the $CH_2CHCHCHN^{\cdot+}$ structure **14** to structure **2**. The other ion structures then first isomerize to the allyl cyanide radical cation according to reactions similar to those in the isomerization of unsubstituted alkene radical cations [9]. This leads to the reaction scheme shown in Fig. 4. In addition to the reactions in Fig. 4, we have also considered some

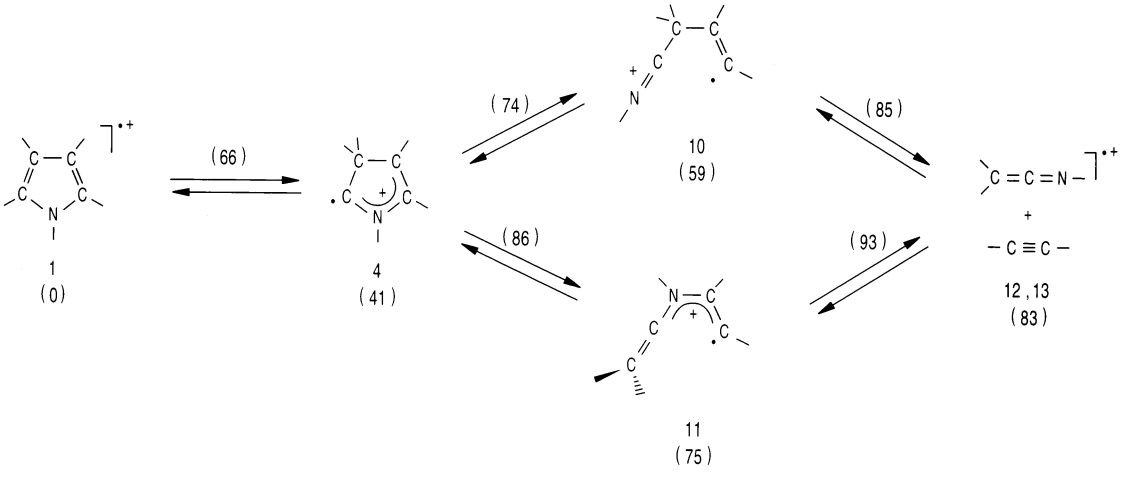

Fig. 2. Reaction scheme for dissociation of the pyrrole radical cation.

Table 2
ROHF, ZPE, and MRCI energies of the different radical cation structures and transition states in Fig. 2 and relative MRCI energies in kcal mol^{-1} corrected for the ZPE at the ROHF or CASSCF level scaled by a factor of 0.89

	ROHF	ZPE	MRCI	ΔE
Pyrrole **1**	−208.596 547	0.087 854	−209.052 045	0
4	−208.535 616	0.087 778	−208.986 604	41.0
10	−208.503 648	0.082 508	−208.953 899	58.6
11	−208.479 276	0.082 765	−208.927 208	75.5
12				
Minimum	−208.463 971	0.075 597	−208.916 729	78.1
7.5 Å	−208.457 904	0.074 824		
10.0 Å	−208.457 232	0.074 824		
15.0 Å	−208.456 895	0.074 821	−208.907 773	83.3
20.0 Å	−208.456 832	0.074 795		
13				
Minimum	−208.473 333	0.076 067	−208.929 087	70.6
7.5 Å	−208.457 715	0.074 845		
10.0 Å	−208.457 146	0.074 793		
15.0 Å	−208.456 874	0.074 780	−208.907 603	83.3
20.0 Å	−208.456 814	0.074 768		
$T_{1,4}$	−208.489 398	0.084 201	−208.943 475	66.1
$T_{4,10}$[a]	−208.442 297	0.081 270	−208.928 980	73.5
$T_{4,11}$[a]	−208.433 752	0.082 028	−208.909 408	86.3
$T_{10,12}$	−208.435 870	0.076 583	−208.906 238	85.2
$T_{11,13}$	−208.413 100	0.075 084	−208.891 964	93.3

[a] Optimized in a CASSCF calculation with 3 electrons in 4 orbitals. The ROHF energy for this geometry and the ZPE at the CASSCF level.

other possibilities. The first is a 1,2-hydrogen shift in the CHCN unit of the cyclopropyl cyanide radical cation followed by ring opening and a 1,3-hydrogen shift to the methacrylonitrile structure **21**. The reason for studying this process was that the first step in the reaction is comparable to a hydrogen shift in the propionitrile radical cation observed before [16]. The relative energy of the cyclic intermediate (100 kcal mol^{-1}), however, appeared to be already higher than the barrier for ring opening of the cyclopropyl cyanide radical cation to structure **22** included in Fig. 4. This process, therefore, was neglected. Another possibility not included in Fig. 4 is an isomerization of the crotonitrile radical cation **17** to the methacrylonitrile structure **19** via the (unstable) carbene ion structure $CH_3CH(CN)CH$ by first a shift of the methyl or cyano substituent and then a hydrogen shift. The relative energy of this intermediate was also significantly higher (106 kcal mol^{-1}) than the energies of the transition states in Fig. 4. The energy difference with the other processes is even higher than for the similar reaction in the butene case [9].

The results of the calculations (Table 3 and Fig. 4) are comparable to those obtained for the butene radical cations in [9] but also show some interesting differences due to the replacement of a methyl substituent by a CN group. In the following especially these differences will be discussed in more detail.

Similar to the isomerization pathways from the 1-butene to the 2-butene radical cation, the isomerization of the allyl cyanide ion **15** to the crotonitrile structure **17** via the substituted trimethylene radical cation **18** proceeds at lower energies than the isomerization via the substituted carbene ion structure **16**.

In the (unstable) $CH_2CH_2CHCH_3^{\cdot+}$ intermediate in the butene case the charge is localized on the $CHCH_3$ group. As a result the ion isomerizes to the linear ion structure of highest energy (1-butene) without a barrier. Structure **18** could be optimized at the ROHF/4-31G level. A Mulliken population analysis gave the unpaired electron localized on the CHCN group and the charge on the unsubstituted CH_2 unit. From this result one expects that, in this case, structure **18** will isomerize via a very low barrier to the structure of

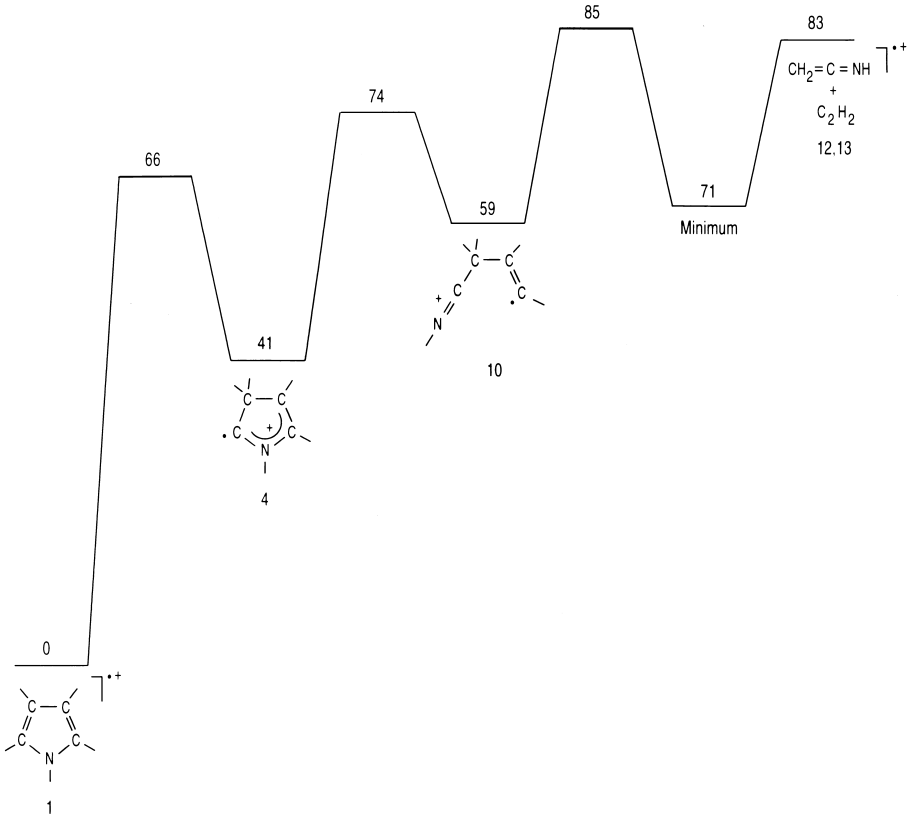

Fig. 3. Final energy diagram for the dissociation of the pyrrole radical cation.

lowest energy, the crotonitrile radical cation **17**. In fact, all attempts to optimize **18** at the ROHF/DZP level did not give a stable ion structure but produced the crotonitrile structure **17**. In order to get an acceptable value for the energy in the neighborhood of **18**, we therefore performed partial optimizations by first optimizing all geometrical parameters except those for the hydrogen atoms on the central carbon atom and then optimizing only the parameters for these hydrogens. The resulting energy values are those given in Table 3. Clearly, it is useless to try to find a geometry for the hypothetical transition state $T_{17,18}$.

For an isomerization of **18** to the allyl cyanide ion **15** a substantial change in the distribution of the charge and the unpaired electron is needed and, similar to the isomerization of $CH_2CH_2CHCH_3^{\cdot+}$ to the 2-butene structure in [9], an optimization of the transition state $T_{15,18}$ was only possible after a switch from ROHF to CASSCF calculations with an active space of 3 electrons in 4 orbitals. The final wave function, however, was close to a single Slater determinant.

Further differences with the C_4H_8 case were obtained for the geometry of the cyclopropyl cyanide radical cation and the isomerization of the linear radical cations to the methacrylonitrile structure. For the methylcyclopropane radical cation three stationary points were found in [9]. In agreement with previous experimental work [18], the geometry of lowest energy of the methylcyclopropane radical cation is asymmetric and has one very long C–C bond connecting the substituted carbon atom with one of the other carbon atoms in the ring. The other stationary points are symmetric transition states. One has two long C–C bonds and the other one a very long C–C bond opposite to the substituted carbon atom. Their relative

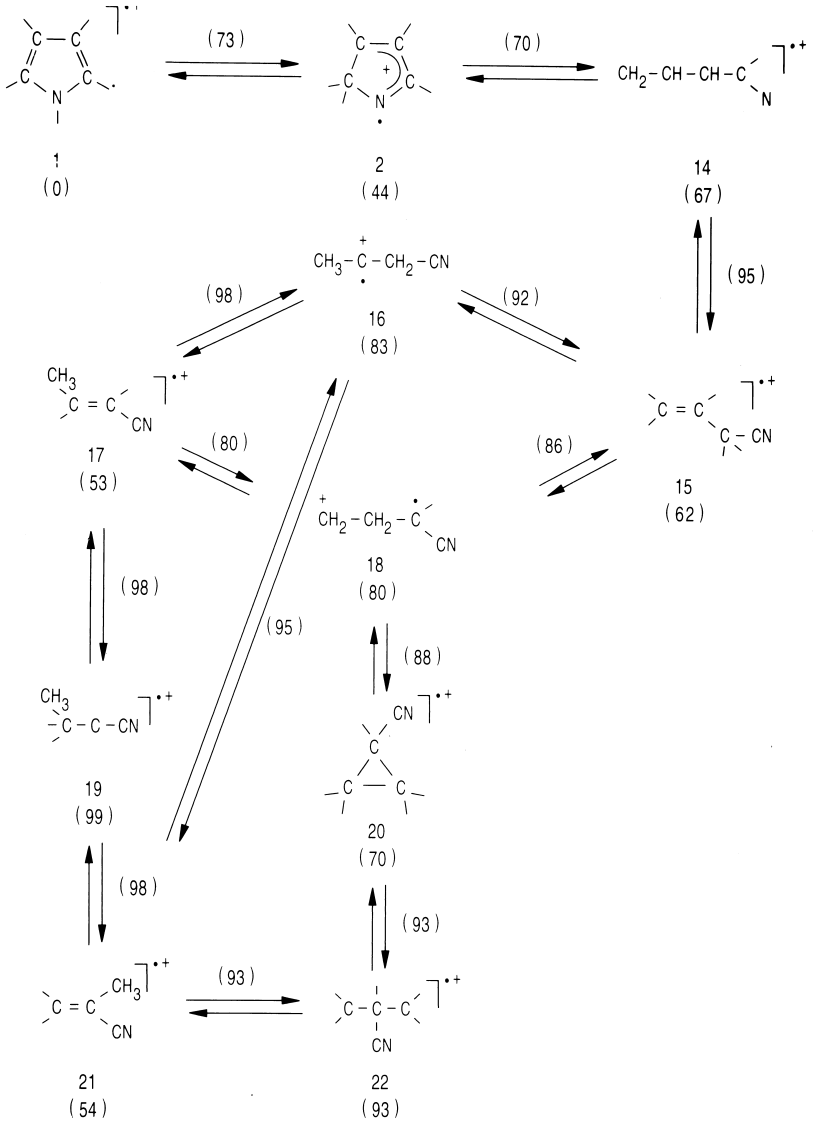

Fig. 4. Reaction scheme considered for the isomerization of C_4H_5N radical cations.

energies are 3.7 and 5.4 kcal mol^{-1}, respectively. For the cyclopropyl cyanide radical cation similar stationary points were found (Fig. 5). At the ROHF level, the relative energies of these geometries are similar to the methylcyclopropane case (see Table 3). According to a calculation of the force constants, **20B** and **20C** are minima and **20A**, the geometry with two long C–C bonds, is a transition state. The vibration corresponding with the single negative force constant shows a symmetry-lifting motion of the ring carbons. This, presumably, is due to an artificial symmetry breaking [19–21] at the ROHF level because after the additional MRCI calculation **20A** appears to be the geometry of lowest energy (Table 3).

For the $CH_2CH(CH_3)CH_2$ radical cation three rather different stationary points were found in [9]. One has a very long C–H bond on the central carbon atom and is a transition state for a hydrogen shift in

Table 3
ROHF, ZPE, and MRCI energies of the different radical cation structures and transition states in Figs. 4 and 5 and relative MRCI energies in kcal mol^{-1} corrected for the ZPE at the ROHF or CASSCF level scaled by a factor of 0.89; experimental values [17] for the relative energies are 58, ≤57, 54, and 65 kcal mol^{-1} for the allyl cyanide, crotonitrile, methacrylonitrile and cyclopropyl cyanide radical cations, respectively

	ROHF	ZPE	MRCI	ΔE
Pyrrole **1**	−208.596 547	0.087 854	−209.052 045	0
2	−208.532 001	0.086 294	−208.979 764	44.5
14	−208.499 624	0.083 169	−208.940 932	67.1
Allyl cyanide				
15	−208.508 110	0.082 687	−208.948 079	62.4
16	−208.467 030	0.079 683	−208.911 720	83.5
Crotonitrile				
17	−208.511 454	0.082 356	−208.962 127	53.4
18	−208.471 939	0.078 588	−208.915 580	80.5
19	−208.440 588	0.080 583	−208.888 369	98.6
Cyclopropylcyanide				
20A	−208.480 082	0.082 678	−208.935 357	70.3
20B	−208.483 200	0.083 020	−208.931 983	72.6
20C	−208.476 701	0.082 291	−208.922 332	78.3
Methacrylonitrile				
21	−208.509 297	0.082 244	−208.957 387	56.3
22A	−208.433 506	0.080 348	−208.896 529	93.4
22B	−208.417 202	0.081 187	−208.880 434	104.0
$T_{1,\,2}$	−208.469 566	0.081 817	−208.930 327	73.0
$T_{2,\,14}$	−208.482 163	0.083 266	−208.935 776	70.4
$T_{14,\,15}$	−208.431 322	0.078 687	−208.893 130	94.6
$T_{15,\,16}$	−208.449 365	0.078 960	−208.897 115	92.3
$T_{16,\,17}$	−208.439 949	0.078 175	−208.887 862	97.6
$T_{16,\,21}$	−208.438 019	0.080 429	−208.893 248	95.5
$T_{15,\,18}$[a]	−208.454 901	0.076 989	−208.906 009	85.6
$T_{17,\,19}$	−208.436 703	0.079 193	−208.887 897	98.2
$T_{19,\,21}$	−208.438 826	0.081 169	−208.889 856	98.0
$T_{18,\,20}$	−208.466 632	0.080 068	−208.904 252	88.4

[a] Geometry optimized in a CASSCF calculation with an active space of 3 electrons in 4 orbitals. The ROHF energy for the final geometry and the ZPE at the CASSCF level.

the 1-butene radical cation. The second geometry has a very long C–CH_3 bond and is a transition state for a methyl shift in the isobutene radical cation. The third geometry, finally, has rather normal bond lengths. Its energy, however, is significantly higher than that of the other geometries and this structure appeared to be a transition state between the other two geometries. In order to avoid an artificial symmetry breaking, the present calculations on the $CH_2CH(–CN)CH_2$ radical cation **22** were done in C_s symmetry. Two different ion geometries were found. A calculation of the force constants showed that both are (local) minima. The first one (**22A**) has a very long C–H bond on the central carbon atom (Fig. 6). When the optimization was started with a geometry similar to the one with the long C–CH_3 bond in the $CH_2CH(CH_3)CH_2$ radical cation, the result was an ion geometry (**22B**) with rather normal bond lengths but a significantly higher energy (Table 3). When the optimization of **22A** was repeated without symmetry, the ion geometry changed drastically and the final result was the methacrylonitrile structure **21**. If the symmetry was maintained except for the dihedral angles of the terminal CH_2 groups, the optimization produced the cyclopropyl cyanide radical cation **20**. Our conclusion thus is that **22A** is not a stable ion structure but at most a shallow local minimum in a transition region between the cyclopropyl cyanide **20** and methacrylo-

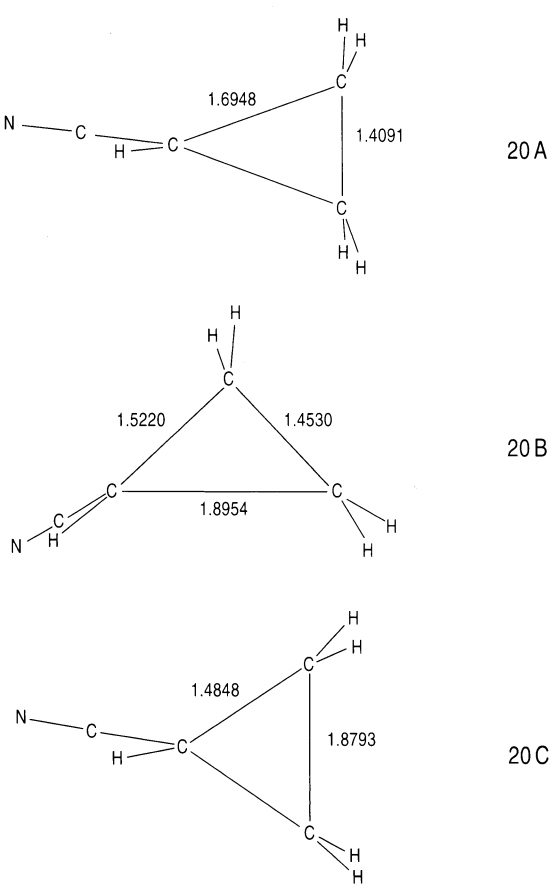

Fig. 5. Projection of the ion geometries obtained for the cyclopropyl cyanide radical cation.

nitrile **21** ion structures. For this reason no further attempts were made to find clearly defined transition states $T_{20,22}$ and $T_{21,22}$. The present conclusion about the instability of **22A** toward a ring closure to the cyclopropyl cyanide ion is somewhat in contrast to the similar reaction in the C_4H_8 case where the barrier is 8 kcal mol^{-1} but in agreement with the result obtained for pentene ions [9].

The isomerization of the methacrylonitrile radical cation **21** to the linear ion structures can take place in three different ways. According to the results in [9] the pathway of lowest energy in the butene case is a methyl shift to a carbene ion structure, similar to structures **16** and **19**, followed by a hydrogen shift whereas for pentene radical cations the pathway of lowest energy proceeds via a substituted cyclopropane radical cation. The present results indicate that the reaction via structure **19**, a methyl shift followed by a hydrogen shift has a higher barrier (45 kcal mol^{-1}) than a shift of the cyano substituent followed by a hydrogen shift via structure **16** (41 kcal mol^{-1}) or the reaction structure via **22** (39 kcal mol^{-1}). The difference between these latter values is perhaps too small to arrive at a definite conclusion about the pathway of lowest energy. In the energy diagram in Fig. 7 we assume, however, that the isomerization of the methacrylonitrile radical cation to a linear ion structure proceeds via the cyclopropyl cyanide radical cation **20**. In this diagram we have furthermore only included the classical ion structures and the lowest barriers connecting them.

4. Comparison with the photodissociation experiments

As described in Sec. 1, most of the radical cations, studied in the photodissociation experiments [4], isomerize in part to the pyrrole ion structure. As shown in Table 3 and Figs. 1 and 7, the highest barrier in these isomerizations has a relative energy of 94.6 kcal mol^{-1} = 4.10 eV. This value is higher than the dissociation limit of 3.43 eV [2]. In previous work on the benzene radical cation, it has been shown that dissociation of the benzene ion is in strong competition with stabilization by infrared emission [22]. This has important consequences, e.g. for the 1,5-hexadiyne radical cation, which isomerizes to the benzene structure without a barrier [8,23]. The resulting benzene ion has an internal energy above the dissociation limit. Stable benzene ions can nevertheless be formed by charge exchange ionization of 1,5-hexadiyne at internal energies far above the dissociation limit of 3.88 eV [24]. For example, according to the calculations reported in [24], half of the benzene ions are stabilized at an internal energy of 4.4 eV. Because the dissociation limit of the pyrrole radical cation is nearly as high as that of the benzene radical cation, it seems quite likely that, also in the present case, the formation of stable pyrrole ions by

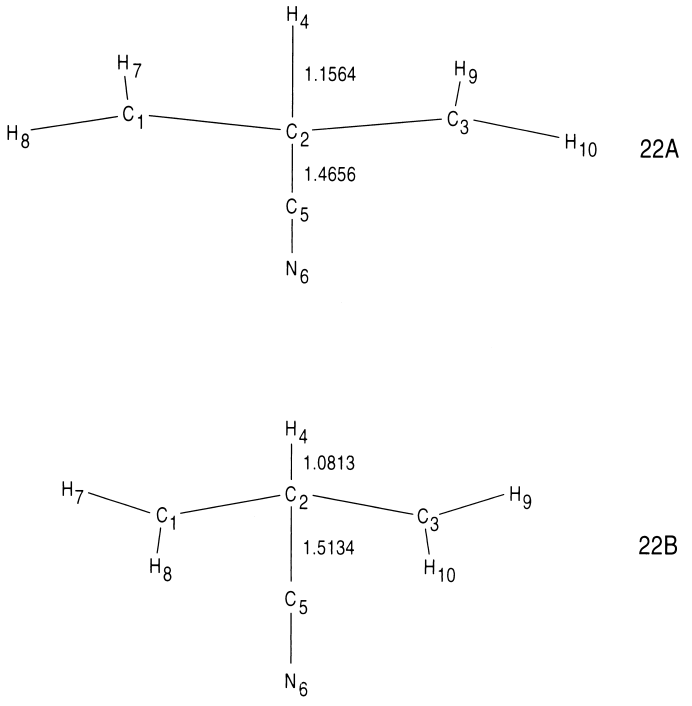

Fig. 6. Projection of the ion geometries obtained for the $CH_2CH(CN)CH_2$ radical cation **22**. The dihedral angles for **22A** and **22B**, respectively, are H_7–C_1–C_2–C_5: 184.5° and 274.7°, H_7–C_1–C_2–H_4: 73.5° and 27.5°, H_8–C_1–C_2–C_5: 13.6° and 84.6°, H_8–C_1–C_2–H_4: 262.6° and 197.4°.

isomerization of the other precursors should be ascribed to infrared radiative stabilization. This seems to be in contrast with the Rice-Ramsperger-Kassel-Marcus (RRKM) calculations on the dissociation of the pyrrole radical cation in [2], which are based on a "loose" transition state looking like structure **10**. Structure **10**, however, is separated from the pyrrole radical cation by two high barriers (Fig. 3). It is possible, therefore, that infrared radiative cooling is not in competition with the final dissociation but with the isomerization to structure **10**.

It is of course difficult to compare the present results with the ion fractions obtained in the photodissociation experiments in [4] because the internal energy after ionization at 16 eV is not known. According to these experiments 6% of the ions from crotonitrile isomerize to the pyrrole ion structure whereas the ions from methacrylonitrile retain the structure of the parent neutral molecule although an isomerization of a small ion fraction to the pyrrole structure could not be ruled out. The energy differences in the final energy diagram in Fig. 7 agree quite well with these conclusions. Also, an isomerization of 30% of the ions from allyl cyanide to the pyrrole structure and of 45% to the crotonitrile structure is understandable on the basis of the energy diagram. Similar conclusions, however, do not hold for the ions from cyclopropyl cyanide. According to the experimental results, 15% of the ions isomerize to the pyrrole structure while the remaining fraction of 85% retains the structure of the parent neutral molecule. This seems to be in conflict with the energy values in Fig. 7 where the barriers for an isomerization to the pyrrole and crotonitrile ion structures are 25 and 18 kcal mol^{-1}, respectively. In addition, the structure of the cyclopropyl cyanide radical cation is very different from that of the neutral molecule. For this reason we have compared the MRCI energies of the different ion structures with the values after vertical ionization. The results in Table 4 show that for cyclopropyl

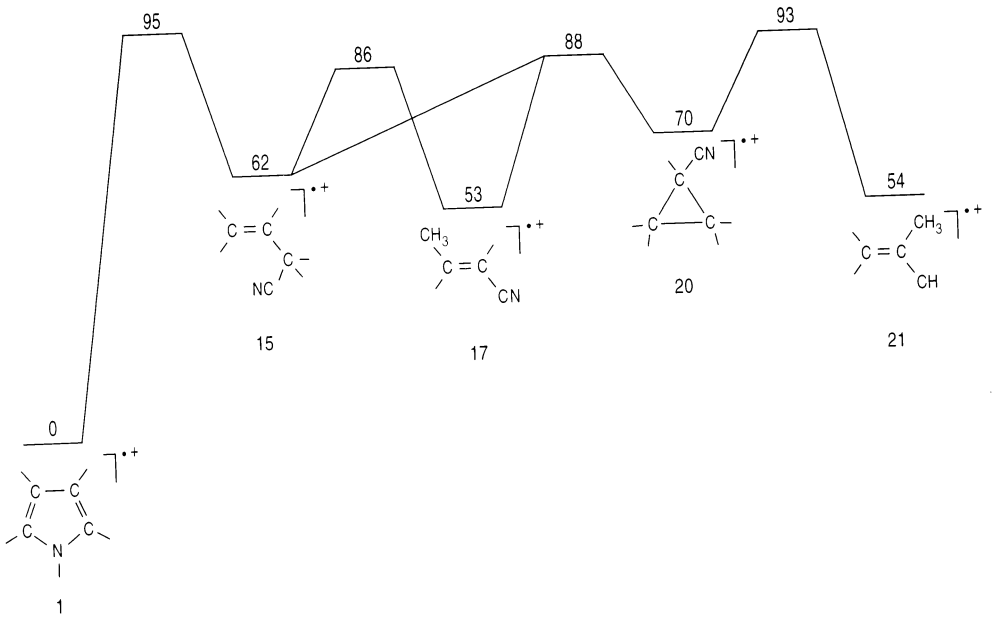

Fig. 7. Final energy diagram for the isomerization of C_4H_5N radical cations.

cyanide the calculated difference between the vertical and adiabatic ionization energy is 23 kcal mol^{-1} which is higher than the barrier of 18 kcal mol^{-1} for isomerization to the crotonitrile radical cation. In [4], the cyclopropyl cyanide radical cation is distinguished from the other ion structures by ion/molecule reactions which show a unique CH_2 transfer. Also, the photodissociation spectra show differences but the difference with the spectrum of the crotonitrile radical cation is mainly in the observed photodissociation rates and not in the position of the maximum in the visible region (see Figs. 3 and 4 in [4]). This could indicate that, for a large part, C_4H_5N radical cations from cyclopropyl cyanide are highly vibrationally excited crotonitrile ions which part of the time have the structure of the CH_2CH_2CHCN ion **18** (see Fig. 4). This may explain both the similarity of the photodissociation spectra and the reactivity by CH_2 transfer in ion/molecule reactions. Further experiments will be necessary to solve this problem.

Table 4
MRCI energies after vertical and adiabatic ionization and energy differences in kcal mol^{-1}

	Vertical	Adiabatic	ΔE
Pyrrole **1**	−209.042 599	−209.052 045	5.9
Allyl cyanide **15**	−208.937 138	−208.948 079	6.9
Crotonitrile **17**	−208.951 222	−208.962 127	6.9
Methacrylonitrile **21**	−208.948 035	−208.957 387	5.9
Cyclopropyl cyanide **20**	−208.898 375	−208.935 357	23.2

References

[1] J. van Thuijl, J.J. van Houte, A. Maquestiau, R. Flamang, C. DeMeyer, Org. Mass Spectrom. 12 (1977) 196.
[2] G.D. Willett, T. Baer, J. Am. Chem. Soc. 102 (1980) 6774.
[3] H. Sakurai, K.R. Jennings, Org. Mass Spectrom. 16 (1981) 393.
[4] M.W.E.M. van Tilborg, J. van Thuijl, W.J. van der Hart, Int. J. Mass Spectrom. Ion Processes 54 (1983) 299.
[5] W.J. van der Hart, J. Am. Soc. Mass Spectrom. 6 (1995) 513.
[6] W.J. van der Hart, J. Am. Soc. Mass Spectrom. 7 (1996) 731.
[7] W.J. van der Hart, J. Am. Soc. Mass Spectrom. 8 (1997) 594.
[8] W.J. van der Hart, J. Am. Soc. Mass Spectrom. 8 (1997) 599.
[9] W.J. van der Hart, J. Am. Soc. Mass Spectrom. 10 (1999) 575.
[10] T.H. Dunning Jr., P.J. Hay, Modern Theoretical Chemistry, H.F. Schaefer III (Ed.), Plenum, New York, 1977, Vol. 3, p. 1.
[11] M.F. Guest, P. Fantucci, R.J. Harrison, J. Kendrick, J.H. van Lenthe, K. Schoeffel, P. Scherwood, GAMESS-UK User's Guide and Reference Manual, Revision C.O, Computing for Science (CFS) Ltd., Daresbury Laboratory, Daresbury, UK, 1992.
[12] M.J. Frisch, G.W. Trucks, H.B. Schlegel, P.M.W. Gill, B.G.

Johnson, M.A. Robb, J.R. Cheeseman, T. Keith, G.A. Petersson, J.A. Montgomery, K. Raghavachari, M.A. Al-Laham, V.G. Zakrzewski, J.V. Ortiz, J.B. Foresman, J. Cioslowski, B.B. Stefanov, A. Nanayakkara, M. Challacombe, C.Y. Peng, P.Y. Ayala, W. Chen, M.W. Wong, J.L. Andres, E.S. Replogle, R. Gomperts, R.L. Martin, D.J. Fox, J.S. Binkley, D.J. Defrees, J. Baker, J.P. Stewart, M. Head-Gordon, C. Gonzalez, and J.A. Pople, GAUSSIAN 94, Revision B.1, Gaussian, Inc., Pittsburgh, PA, 1995.

[13] J. Dillen, Program No. QCMP 12010, Quantum Chemistry Program Exchange, Indiana University, Bloomington, IN 47405, 1992.

[14] R.J. Buenker, R.A. Philips, J. Mol. Struct. (Theochem.) 123 (1985) 291.

[15] S.T. Elbert, E.R. Davidson, Int. J. Quantum Chem. 8 (1974) 857.

[16] C.B. Theissling, N.M.M. Nibbering, S. Meyerson, Org. Mass Spectrom. 11 (1976) 838.

[17] S.G. Lias, J.E. Bartmess, J.F. Liebman, J.L. Holmes, R.D. Levin, W.G. Mallard, J. Phys. Chem. Ref. Data (Suppl 1) 17 (1988).

[18] X-Z. Qin, F. Williams, Tetrahedron 42 (1986) 6301.

[19] P.O. Löwdin, Adv. Chem. Phys. 2 (1959) 207.

[20] P.S. Bagus, H.F. Schaeffer III, J. Chem. Phys. 56 (1972) 224.

[21] A.D. McLean, B.H. Lengsfield III, J. Pacansky, Y. Ellinger, J. Chem. Phys. 83 (1985) 3567.

[22] S.J. Klippenstein, J.D. Faulk, R.C. Dunbar, J. Chem. Phys. 96 (1993) 243.

[23] C. Lifshitz, N. Ohmichi, J. Phys. Chem. 93 (1989) 6329.

[24] W.J. van de Guchte, W.J. van der Hart, L.J. de Koning, N.M.M. Nibbering, R.C. Dunbar, Int. J. Mass Spectrom. Ion Processes 123 (1993) 11.